STED Microscopy: Different Approaches and Applications

Katrin I. Willig, PhD,[1] Lars Kastrup, PhD,[1]
U. Valentin Nägerl, PhD,[2] and Stefan W. Hell, PhD[1]

[1]Department of NanoBiophotonics
Max Planck Institute for Biophysical Chemistry
Göttingen, Germany

[2]Institut National de la Santé et de la Recherche Médicale U862
Université Victor Segalen Bordeaux 2
Bordeaux, France

NOTES

Introduction

Until recently, it was widely accepted that lens-based (far-field) optical microscopes cannot visualize details much finer than about half the wavelength of light. Therefore, to image fine details as of densely packed synaptic vesicles or the synaptic cleft, electron microscopy was always the technique of choice. In the last two decades, however, a family of light microscopy techniques has emerged that breaks through the diffraction limit which was established by Abbe (1873).

STED was the first concrete and feasible concept showing that, in fluorescence microscopy, the diffraction barrier can be broken. STED stands for Stimulated Emission Depletion Microscopy and was introduced in 1994 (Hell and Wichmann, 1994). It is now viewed as part of a family of concepts that utilize reversible saturable optical (fluorescence) transitions, which was named RESOLFT for short (Hell et al., 2003, 2009). All these concepts have in common that the fluorescent marker is switched between two distinct, interchangeable states *A* and *B*, whereby one of these states is fluorescent and at least one of the transitions between *A* and *B* can be driven by light.

Recently, RESOLFT microscopy was complemented by powerful methods that are based on the sequential stochastic switching of individual photoactivatable fluorophores in wide-field illumination (Betzig et al., 2006; Hess et al., 2006, 2009; Rust et al., 2006). The photochromic molecules are switched to a conformational state, leading to m >> 1 consecutive photon emissions and allowing the calculation of the position of individual fluorophores.

The following sections of this chapter explain the basic idea of STED, which led to a modification of Abbe's equation describing the diffraction limit. It then focuses on the STED setup and different approaches to simplify the equipment for a STED microscopy setup, e.g., by using simple continuous wave lasers or a supercontinuum light source. Finally, it discusses an application of STED microscopy to neuroscience.

Principles of STED Microscopy

In a spot-scanning (nonconfocal) fluorescence microscope, the resolution in the focal plane can be described by the spatial extent of the fluorescing area, which in turn is equal to the excitation area $h_{exc}(r)$. Because of diffraction, $h_{exc}(r)$ is a blurred spot with a full width at half-maximum (FWHM) of $\Delta r = \lambda/2n \sin\alpha$ (Born and Wolf, 2002), with λ, n, and α denoting the wavelength of the focused light, the refractive index, and the semi-aperture angle of the objective lens, respectively.

The basic idea behind scanning STED microscopy is to confine the fluorescence emission of fluorescent markers to a region that is much smaller than that covered by the diffraction-limited excitation spot. Therefore, a second, red-shifted beam (called the STED beam) is applied that has the ability to annihilate the molecular excitation and thereby prevent the molecules from fluorescing. The focal spatial extent of the STED beam is usually shaped like a doughnut in order to de-excite molecules only in the outer region of the excitation spot. The STED photons act primarily on the excited state S_1, inducing stimulated emission down to a vibrational sublevel of the ground state S_0^{vib} (Fig. 1, left). Subpicosecond vibrational decay empties S_0^{vib}, so repumping into S_1 is largely ineffective. STED microscopy has been implemented mostly with pulsed beams, whereby the STED pulses of typical 0.1–1.0 ns duration have followed (shorter) excitation pulses. By the time the STED pulse has vanished, the population of the S_1 is $N(h_{STED}) = N0 \exp(-\sigma h_{STED})$, where N_0 is the initial population, $\sigma \approx 10^{-16}$ cm^2 the cross-section for stimulated emission, and $h_{STED}(r)$ is the point-spread function (PSF) of the STED pulse in photons per area per pulse. This formula assumes that the STED pulse is shorter than the fluorescence lifetime, which is a few nanoseconds for organic dyes. Hence, the fluorescence is reduced by a factor $\eta(h_{STED}) = \exp(-\sigma h_{STED})$.

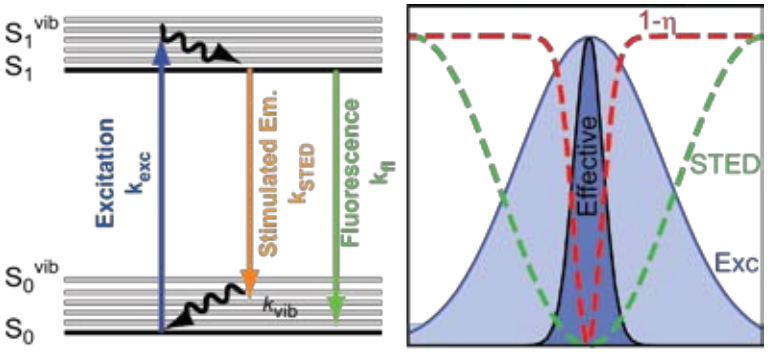

Figure 1. Left, Jablonski diagram showing the energy states of a fluorescent molecule. Right, Breaking the diffraction barrier using STED. Normalized intensity profiles of the excitation PSF h_{exc}, STED PSF h_{STED}, De-excitation probability (1-η) and effective PSF h_{eff}.

NOTES

Using a doughnut-shaped STED pulse with a local zero ($h_{STED}(0) = 0$) implies that the fluorescence emission is unaffected at $r = 0$ but is increasingly suppressed with increasing r (Fig. 1, right). Thus, the STED PSF confines the fluorescence emission to a region that is much narrower than the excitation spot. The effective PSF h_{eff} can be shown to scale with the STED intensity according to the following formula:

$$\Delta r \cong \frac{\lambda}{2n\sin\alpha\sqrt{1+\zeta}} \qquad \text{(Eq. 1)},$$

where the intensity I is given as the "saturation factor" $\zeta = I/I_s$. That is, it is given in multiples of the saturation intensity I_s at which the fluorescence drops to 1/e of its initial value. I_s is characteristic of the dye used. Scanning this reduced focal spot through the sample yields images of subdiffraction resolution.

Setting Up STED for Live Cell Imaging

Figure 2 shows a typical setup of a STED microscope used for live-cell imaging of yellow fluorescent protein (YFP)–expressing samples. For excitation, a laser diode (PicoTA [Picoquant, Berlin]) emitting pulses of 70 ps at 490 nm was used. Each excitation pulse was followed directly by a red-shifted STED pulse. The STED pulses of 80 MHz repetition rate were generated by a Titanium Sapphire (Ti:Sapphire) laser (Mai Tai, Spectra Physics, Mountain View, CA) emitting in the far-red spectrum, which was converted to visible light (STED of YFP: 590 nm) by an optical parametric oscillator (OPO, APE, Berlin, Germany). The ~ 200 fs pulses emitted by the OPO were stretched to ~300 ps by guiding the light through a 100 m long polarization-preserving fiber (OZ Optics [Ottawa, Ontario, Canada]). In order to avoid nonlinear effects in the fiber, the STED pulses were prestretched by guiding them through (SF6) glass before fiber coupling. To synchronize both the excitation and the STED laser, the excitation laser was triggered using the output signal of the photo diode of the Mai Tai. To adjust the temporal delay of the STED pulse with regard to the excitation pulse, we used a custom-made delay unit with a precision of 10 ps.

After the fiber, the collimated STED light passes through a patterned phase plate (vortex pattern, RPC Photonics, Rochester, NY) and is subsequently overlaid with the excitation beam using a dichroic mirror. The profile of the phase plate is fabricated such that the maximal thickness of the polymer corresponds to a phase retardation of 2π for the STED wavelength employed. After focusing through the objective lens (NA 1.4 Oil immersion, 100× PL APO, Leica [Wetzlar, Germany]), the PSF gives the intensity distribution in the focal plane. The PSF of the excitation beam is a blurred, diffraction-limited spot, whereas the PSF of the STED beam shows a doughnut-shaped, albeit diffraction-limited intensity pattern. The center of the doughnut PSF is practically of zero intensity if the STED beam is circularly polarized. Circular polarized light is achieved by introducing a half-wave plate in front of the objective lens.

The fluorescence signal is collected via a multimode optical fiber, which acts as a confocal pinhole. The diameter of the multimode fiber corresponds to 80%

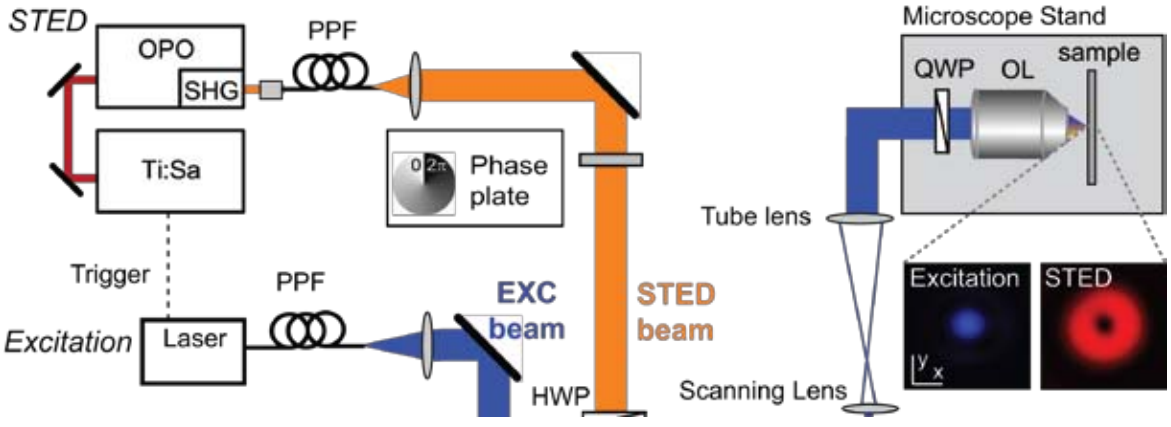

Figure 2. Experimental setup for live-cell STED microscopy. APD, avalanche photo diode; DC, dichroic mirror; HWP, half-wave plate; MMF, multimode optical fiber; OL, objective lens; OPO, optical parametric oscillator; PPF, polarization preserving optical fiber; QWP, quarter-wave plate; SHG, second-harmonic generation; Ti:Sa, Titanium Sapphire laser.

NOTES

of the back-projected Airy disc of the excitation PSF. The fluorescence is filtered from back-reflected laser light by an emission filter in front of the photon-counting detector (APD, PerkinElmer [Salem, MA]) transmitting between 510 nm and 560 nm. Although the resolution in STED microscopy does not depend on the confocal pinhole, a confocal detection does reduce stray and ambient light.

After overlapping the excitation and STED PSFs in all three dimensions, STED images can be recorded either by moving the sample through the focused light spots or by raster scanning the focused beams over the sample. Here, we used a combination of both: The fast scanning axis was recorded by scanning the beam with a resonant mirror (15 kHz, SC-30, EOPC, Glendale, NY), whereas for the second, slow-moving axis, the sample was moved by a piezo stage (P-733, Physik Instrumente, Karlsruhe, Germany).

Simple STED 1: Using Continuous Wave Lasers

STED is a single-photon process and therefore does not rely on pulsed light. For both pulsed and continuous wave (CW) STED, the rate constants are the same, but the boundary conditions are different. CW excitation at a rate k_{exc} populates S_1 with $k_{exc}/ (k_{exc} + k_{fl}) <1$; the fluorescence decay rate $k_{fl} = 1/\tau_{fl}$ is given by the inverse of the lifetime τ_{fl}. Adding a CW STED beam of intensity I merely adds another decay rate $k_{STED} = \sigma I$, yielding a population of S_1 of $N_1 = k_{exc}/ (k_{exc} + k_{fl} + k_{STED}) <1$. σ denotes the molecular cross-section for stimulated emission, and I is the intensity of the STED beam expressed in photons per area per second. Adjusting $k_{STED} >> k_{fl} > k_{exc}$ renders STED predominant, which is the case for $I > (\sigma\tau_{fl})^{-1} = I_s$. The CW power required to produce I_s is given by $P_s = A\, hc/ (\lambda_{STED}\, \sigma\tau_{fl})$, with c, h, and A denoting the speed of light, Planck's constant, and doughnut area, respectively. Applying a greater power P squeezes the spot diameter to subdiffraction dimensions following the square-root law of Equation 1.

Especially in the visible range, expensive laser systems (e.g., Mai Tai and OPO) were traditionally required to operate a STED microscope. Less expensive and easy-to-operate alternatives are therefore highly welcome: CW lasers. Lately, CW lasers have become available that cost only ~10% of the Mai Tai/OPO combination while providing sufficient power for STED microscopy. In addition to their lower cost, CW lasers simplify the STED microscope setup considerably because temporal synchronization of the STED pulses with their excitation counterparts becomes obsolete. Also obsolete is stretching the STED pulse using an optical fiber or optical grating. Another advantage is that the technology behind a low-power CW excitation laser is much simpler and therefore less expensive than a pulsed excitation laser. Basically, if the noise of the laser is low enough, a simple laser pointer can be sufficient for excitation.

For dyes typically used for STED microscopy, P_s is about five times larger than the time-averaged power reported in experiments with pulsed systems. This is easily understood by envisioning the STED pulse being gradually spread outward from the time point of the excitation pulse. Stretching it up to about $\tau_{fl} \approx 3$ ns reduces the peak intensity I by about 12-fold but leaves the STED efficiency largely intact. This is because, when acting well within the time span τ_{fl}, only the amount of photons in the pulse matters, STED being a one-photon process. Spreading the pulse farther out in time, up to the next excitation pulse arriving after τ_{rep}=12.5 ns (for 80 MHz), unduly reduces I. Hence, to maintain I continually (as is inherently required for CW operation), the beam power has to be enlarged by a factor of $\tau_{rep}/\tau_{fl} \approx 4$.

To validate this assumption, Figure 2*A* shows a depletion of S_1 with increasing power P for the CW mode and the standard pulsed mode (Willig et al., 2007). It was measured with a far-red-emitting dye and a Ti:Sapphire laser for the STED beam, which can provide both modes: CW and pulsed (76 MHz). The fluorescence depletion was virtually identical for the pulsed and CW STED modes. The only difference was that the power of the CW beam was ~3.6 times larger than the time-averaged power of the STED pulses. This finding is in agreement with the calculation τ_{rep}/τ_{fl} = 13.15 ns/3.77 ns = 3.5.

By converting the STED focal spot into a doughnut, subdiffraction images can be obtained. Figure 2*B* shows an image of the heavy subunit of neurofilaments in a fixed human neuroblastoma cell, immunologically labeled with an antibody conjugated to Atto647N. In contrast to the confocal image, the CW STED image (P = 423 mW at 750 nm) shows a substructure of separated spots in the axon with a resolution of 52 nm (Willig et al., 2007).

Note, however, that CW STED microscopy is not limited to fixed and/or immunolabeled samples. Figure 2C shows a CW STED image of Citrine-labeled endoplasmic reticulum (ER) tubules in a living PtK2 cell that are as small as ~60 nm (Hein et

NOTES

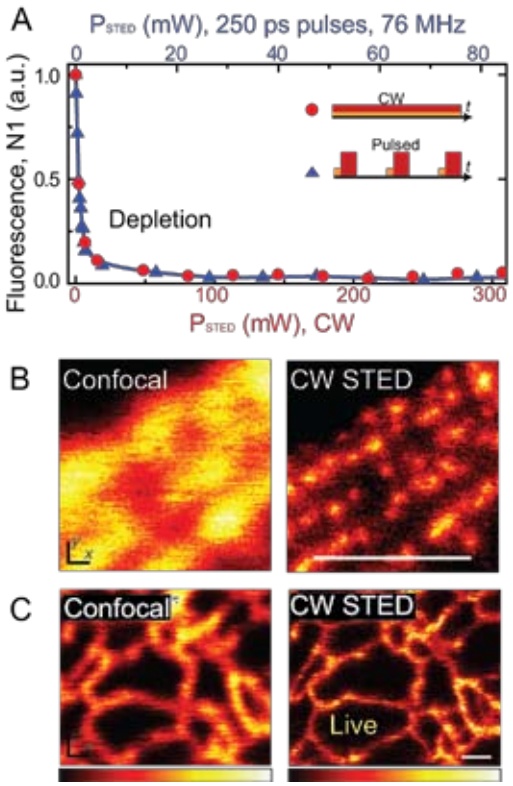

Figure 3. Continuous wave STED microscopy. ***A***, De-excitation of the fluorescence in CW mode coincides with those in the pulsed mode, using 80 ps pulses for excitation and 250 ps pulses for depletion. ***B***, Immunofluorescence-labeled neurofilaments in human neuroblastoma marked by the red-emitting dye Atto647N recorded by CW STED microscopy and for comparison in the confocal mode. CW excitation at 630 nm. Scale bar: 1 µm. (For details, see Willig et al., 2007.) ***C***, Live-cell CW STED and corresponding confocal image of the YFP Citrine targeted to the ER-revealing tubules as small as 60 nm. To de-excite the fluorescence at 592 nm, a small-footprint fiber laser (MPB Communications [Montreal, Quebec, Canada]) was used. Scale bar: 1 µm.

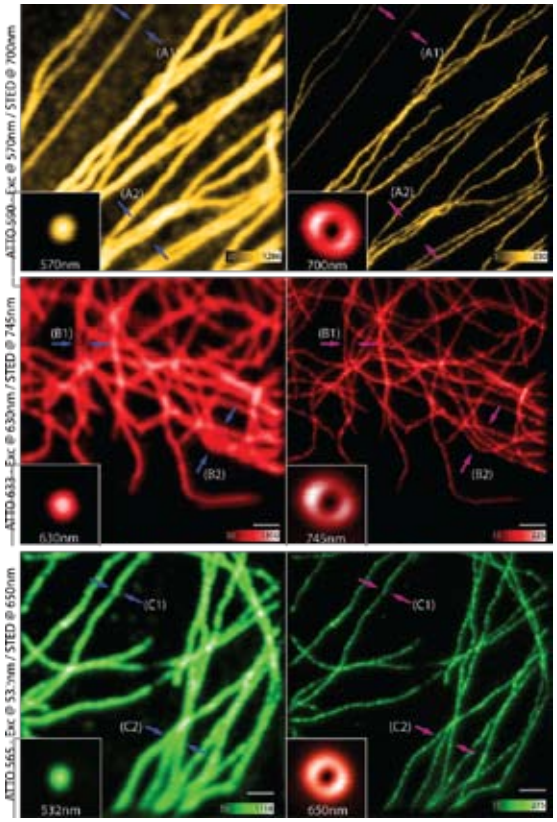

Figure 4. STED microscopy using a supercontinuum light source. Wildanger et al. (2008), their Fig. 3, reprinted with permission. Immunolabeled tubulin fibers imaged with an excitation wavelength of 570 nm (top), 630 nm (middle), and 532 nm (bottom). The comparison between the confocal reference image (left) and the STED image (right) reveals the gain in structural information obtained by STED; note that all images represent raw data. Scale bar: 1 µm.

al., 2008). This demonstrates that fluorescent proteins can also be employed in a CW STED microscope.

Simple STED 2: Supercontinuum Laser Source

Another way to build a compact STED microscope is by using a supercontinuum laser source (Wildanger et al., 2008). By using a laser source that provides light over basically the whole visible spectrum up to the infrared region, STED imaging can be done at different colors. And, because the emission spectrum of the supercontinuum source is so broad, it can be used for excitation and emission simply by sorting out the proper wavelengths. For most fluorophores, the useful spectral bandwidth of a STED pulse typically spans 20 nm. For enhancing the resolution by about a factor of five in the *x* and *y* directions, a pulse energy of ~5 nJ is usually employed. So far, only supercontinuum lasers available with a repetition rate ≤1 MHz produce these high-pulse energies.

One advantage of operating at pulse repetition rates of ~1 MHz is that photobleaching rates are reduced by allowing the fluorophore to relax from excitable, meta-stable dark states (D-Rex) or triplet states (T-Rex), which are involved in photodegradation. Because dark states (in particular, the triplet state) are known to be involved in photobleaching via charge-tunneling or triplet absorption, photobleaching can be reduced simply by avoiding illuminating molecules as long as they are in the triplet state. In D-Rex microscopy, the repetition rate is so low that the time interval between consecutive pulse pairs is larger than the average lifetime of an excited, meta-stable dark state of the fluorophore. Because the

NOTES

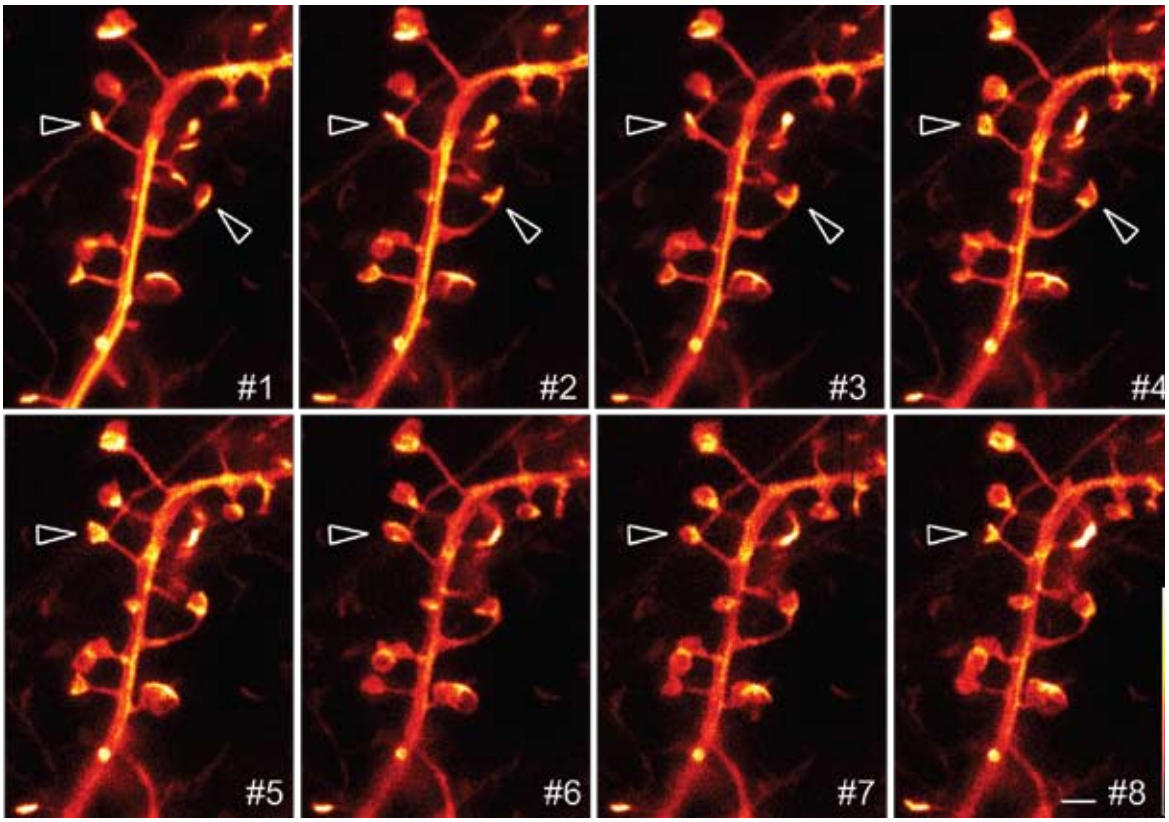

Figure 5. Time-lapse STED imaging of dendritic structures in organotypic hippocampal slices from YFP-transgenic mice. Adapted from Nagerl et al. (2008), their Fig. 3*A*, with permission. Arrows indicate cup-like shapes that are formed over time. Images were acquired at a frame rate of 40 s/frame with a break of several minutes between frames. Scale bar: 1μm.

average lifetime of such dark states is typically in the microsecond range, pulse repetition rates of <1 MHz ensure that the dark states have relaxed by the time the subsequent pulse pair arrives.

Figure 4 shows immunofluorescence-labeled microtubules of a mammalian PtK2 cell. These images were recorded with a home-built STED microscope employing a commercially available supercontinuum source (SC-450 HP [Fianium, Southampton, UK]) at a repetition rate of 1 MHz. Three different colors were chosen for excitation and STED, respectively, to account for the excitation and emission of the three different dyes (ATTO 565/ATTO 590/ATTO 633 [ATTOTEC, Siegen, Germany]). These dyes are customary organic dyes and are not specifically optimized for STED microscopy. All three STED images of the different labeled microtubules in Figure 3 reveal clearly distinct fibers, in contrast to the confocal reference images. The diameter of the fibers in the STED image is 60–80 nm. Thus, the actual resolution of the STED microscope in these images ranges from 30 to 50 nm.

STED Microscopy of Living Dendritic Spines

The structural plasticity of synaptic connections is a key mechanism in the brain whereby neuronal circuits are refined or remodeled during development and by experience. Spines, in particular, which are the dendritic protrusions that form the postsynaptic part of most excitatory synapses in the mammalian brain, display a remarkable degree of structural plasticity. Structural plasticity has been shown to be closely linked to functional changes in the strength of synaptic transmission, such as long-term potentiation (LTP) and long-term depression (LTD).

Spines are ~0.2–2.0 μm in length and therefore can be readily identified by standard light microscopy techniques. However, measuring changes in their shape or size has been difficult, because they are usually smaller than the diffraction limit. For example, fine details such as the width of spine necks (which varies from 40 to 500 nm for spines on CA1 pyramidal neurons) often cannot be resolved by conventional

NOTES

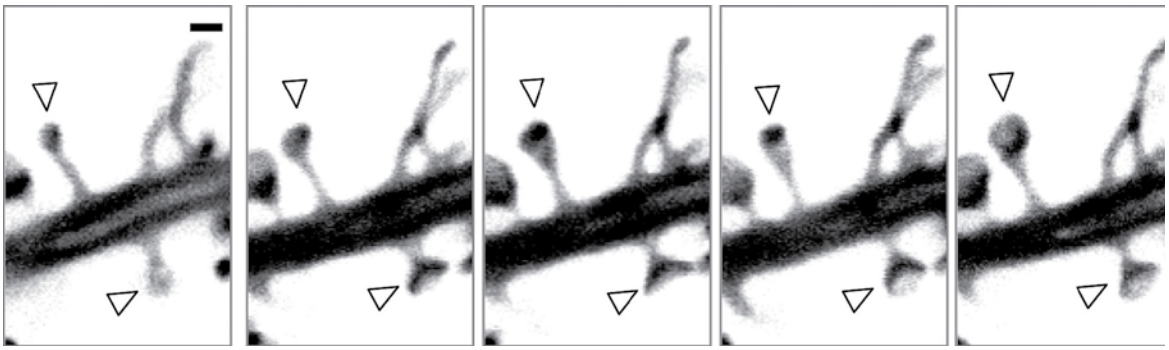

Figure 6. STED imaging of activity-dependent postsynaptic morphological plasticity. Nagerl et al. (2008), their Fig. 4*C*, reprinted with permission. Arrows indicate structural changes in dendritic spines that occurred after plasticity-inducing stimulation using chemical LTP protocol. The first frame was taken before the stimulation. Scale bar: 0.5 µm.

light microscopy. STED microscopy, however, can resolve these details without sacrificing the ability to reveal dynamic biological cellular processes inside living tissue, which is a key advantage of light microscopy (Nagerl et al., 2008).

To demonstrate the power of STED microscopy for imaging dendritic spines, we used YFP-positive CA1 pyramidal neurons in living organotypic hippocampal slices. Hippocampal slices (300 µm thick) were prepared and embedded in a plasma clot on glass coverslips according to standard procedure (Gähwiler, 1981) and incubated for up to two weeks in a roller incubator at 35°C. For the experiments, cultures were transferred into a heated chamber (35°C), where they were maintained in artificial CSF solution. The chamber was custom-made to fit into the microscope stage. Sample handling and preparation followed standard techniques for fluorescence imaging of living specimens and were not altered specifically for STED microscopy.

Figure 5 shows a time-lapse series of STED images (8 out of a total of 20), revealing subtle changes in the shape and position of YFP-labeled dendritic spines. Image series of up to 100 frames could be acquired using a resonant beam scanner without any signs of photodamage (data not shown). To demonstrate the improvement in resolution as compared with confocal microscopy, we measured the full width at half maximum (FWHM) of spine necks. The smallest structures were ~70–80 nm in size, indicating a resolution of better than 70 nm. Because most of the spine necks were broader than 70 nm, the resolution of the microscope was well suited to capture the variability in the width of spine necks. We determined the FWHM of multipixel-line profiles across the narrowest part of the spine necks, which was 129 ± 25 nm in the STED mode and 233 ± 22 nm in the confocal mode.

Beyond resolving structural details, it was also possible to directly observe activity-dependent structural changes in the shape and size of dendritic spines. To induce structural changes, we subjected the slices to chemical LTP, which is a standard protocol for globally potentiating synapses by pharmacologically raising neuronal activity in the entire slice. The arrows in Figure 6 indicate changes in spine shape after inducing chemical LTP.

These examples show that time-lapse imaging using STED microscopy can reveal details of spines in living tissue that are very difficult, if not impossible, to detect by conventional light microscopy techniques. These can now be rigorously quantified for the first time.

References

Abbe E (1873) Beiträge zur Theorie des Mikroskops und der mikroskopischen Wahrnehmung. Arch Mikrosk Anat Entwichlungsmech 9:413-468.

Betzig E, Patterson GH, Sougrat R, Lindwasser OW, Olenych S, Bonifacino JS, Davidson MW, Lippincott-Schwartz J, Hess HF (2006) Imaging intracellular fluorescent proteins at nanometer resolution. Science 313:1642-1645.

Born M, Wolf E (2002) Principles of optics (7th ed). Cambridge, New York, Melbourne, Madrid, Cape Town: Cambridge University Press.

Gähwiler BH (1981) Organotypic monolayer cultures of nervous tissue. J Neurosci Methods 4:329-342.

Hein B, Willig KI, Hell SW (2008) Stimulated emission depletion (STED) nanoscopy of a fluorescent protein-labeled organelle inside a living cell. Proc Natl Acad Sci USA 105:14271-14276.

Hell SW (2009) Microscopy and its focal switch. Nat Methods 6:24-32.

Hell SW, Wichmann J (1994) Breaking the diffraction resolution limit by stimulated-emission–stimulated-emission-depletion fluorescence microscopy. Opt Lett 19:780-782.

Hell SW, Jakobs S, Kastrup L (2003) Imaging and writing at the nanoscale with focused visible light through saturable optical transitions. Appl Phys A 77:859-860.

Hess ST, Girirajan TPK, Mason MD (2006) Ultra-high resolution imaging by fluorescence photoactivation localization microscopy. Biophys J 91:4258-4272.

Nagerl UV, Willig KI, Hein B, Hell SW, Bonhoeffer T (2008) Live-cell imaging of dendritic spines by STED microscopy. Proc Natl Acad Sci USA 105:18982-18987.

Rust MJ, Bates M, Zhuang XW (2006) Sub-diffraction-limit imaging by stochastic optical reconstruction microscopy (STORM). Nat Methods 3:793-795.

Wildanger D, Rittweger E, Kastrup L, Hell SW (2008) STED microscopy with a supercontinuum laser source. Opt Express 16:9614-9621.

Willig KI, Harke B, Medda R, Hell SW (2007) STED microscopy with continuous wave beams. Nat Methods 4:915-918.

NOTES